

# Measuring anomalous $Wtb$ couplings at $e^-p$ collider

---

Sukanta Dutta,<sup>a</sup> Ashok Goyal,<sup>b, \*</sup> Mukesh Kumar<sup>a,b, †</sup> and Bruce Mellado<sup>c, ††</sup>

<sup>a</sup>*SGTB Khalsa College, University of Delhi, Delhi, India*

<sup>b</sup>*Department of Physics & Astrophysics, University of Delhi, Delhi, India*

<sup>c</sup>*University of the Witwatersrand,*

*Private Bag 3, Wits 2050, Johannesburg, South Africa*

*E-mail:* [★agoyal45@yahoo.com](mailto:★agoyal45@yahoo.com), [†mkumar@physics.du.ac.in](mailto:†mkumar@physics.du.ac.in),

[††bmellado@mail.cern.ch](mailto:††bmellado@mail.cern.ch)

**ABSTRACT:** We study the physics potential of the proposed LHeC by estimating the accuracy with which it can measure the anomalous  $Wtb$  couplings in the single anti-top quark production through  $e^-p$  collision. We consider the generic lowest order  $CP$  conserving Lagrangian for the  $Wtb$  interaction which allows a right-handed vector, as well as left- or right-handed tensor couplings. We examine the one dimensional distributions of the various kinematic observables and their asymmetries corresponding to all anomalous couplings in both hadronic and leptonic decay modes of  $W^-$ . We find that the 95% C.L. exclusion contours on the two dimensional plane of anomalous couplings associated with the left- and right-handed vector and tensor currents are sensitive at an order of magnitude of  $\sim 10^{-3} - 10^{-2}$  with  $100 \text{ fb}^{-1}$  data. Further, adoption of the optimum observable method, results in an enhancement in the sensitivity of the left handed anomalous couplings by an order of magnitude and also provides their error correlations.

---

## Contents

<b>1</b>	<b>Introduction</b>	<b>1</b>
<b>2</b>	<b>Single anti-top quark production</b>	<b>7</b>
2.1	Sensitivity in the Hadronic Mode	8
2.2	Sensitivity in the Leptonic Mode	10
<b>3</b>	<b>Estimators and <math>\chi^2</math> analysis</b>	<b>11</b>
3.1	Angular Asymmetries from Histograms	11
3.2	Exclusion contours from bin analysis	14
3.3	Errors and correlations	15
<b>4</b>	<b>Observations and conclusions</b>	<b>18</b>

---

## 1 Introduction

The top quark being the heaviest particle in the Standard Model (SM) provides an excellent opportunity for the study of electroweak symmetry breaking mechanism as well as to provide glimpse of new physics (NP) beyond the SM. The top (anti-top) quark decays almost exclusively in the  $t \rightarrow bW^+$  ( $\bar{t} \rightarrow \bar{b}W^-$ ) channel. As a consequence of its lifetime ( $\sim 10^{-25}$  s), being one order of magnitude smaller than the typical hadronization time scale ( $\sim 10^{-24}$  s), its spin information is transferred to the decay products. The kinematic

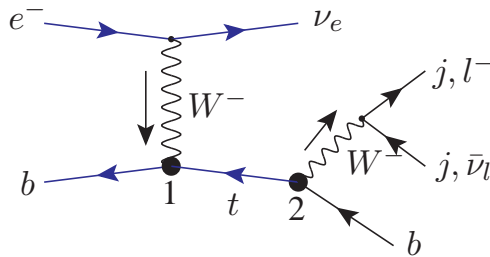


**Figure 1.** Single anti-top quark production through charge current at the  $e$ - $p$  collider. The blobs at vertices 1 and 2 show the effective  $W^-t\bar{b}$  couplings, which includes the SM contribution. Further  $W^-$  decays into hadronic mode via light quarks ( $j \equiv \bar{u}, d, \bar{c}, s$ ) or leptonic mode ( $l^- \equiv e^-, \mu^-$ ) with missing energy.

distributions of decayed particles from top (anti-top) quark provide the information about the  $W^+tb$  ( $W^-t\bar{b}$ ) vertex and associated new physics potentiality with the top (anti-top) quark production mechanism. Within the SM, the  $Wtb$  vertex is purely left-handed, and its

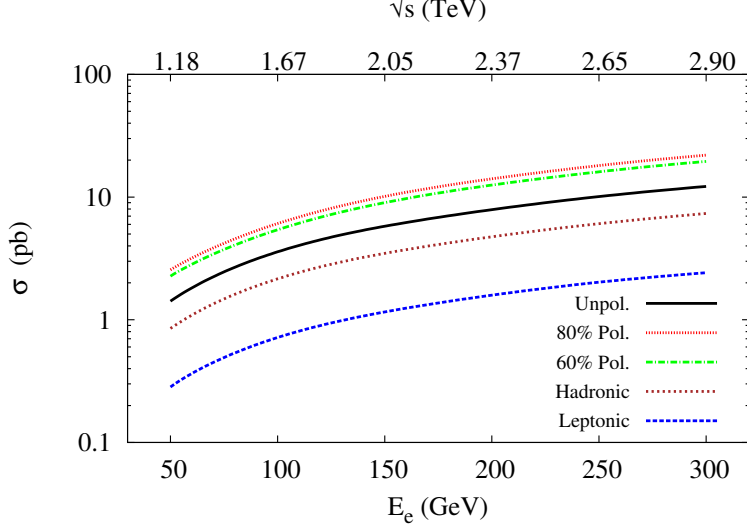


**Figure 2.** Single anti-top quark production cross section at LHeC with the variation of electron energy  $E_e$ , while fixing the proton energy to be  $E_p = 7$  TeV. The top three curves corresponds to the 80% and 60% polarized and unpolarized  $e^-$  beam, respectively. Brown and blue lines (second and first from below, respectively) corresponds to the cross-section with  $W^-$  decaying in the hadronic and leptonic mode, respectively.

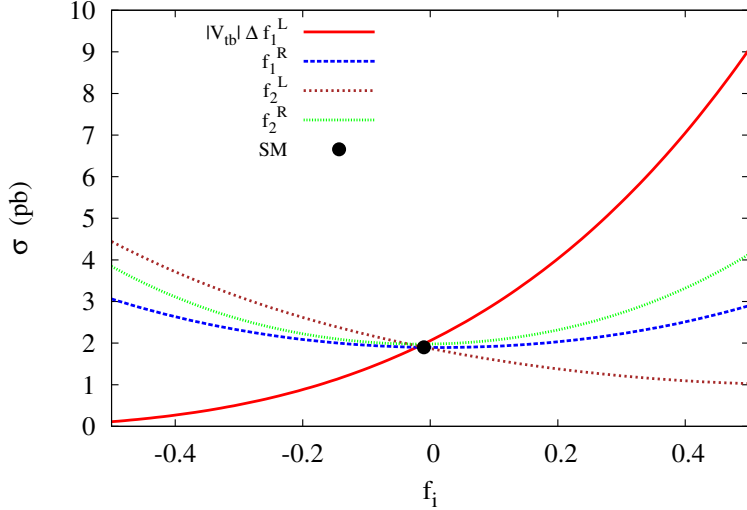


**Figure 3.** Variation of the single anti-top quark production cross section with the effective  $Wtb$  couplings (taken one anomalous coupling at a time with SM) at the production and decay vertices, for fixed  $E_p = 7$  TeV and  $E_e = 60$  GeV.

amplitude is given by the Cabibbo-Kobayashi-Maskawa (CKM) matrix element  $V_{tb}$ , related to weak interaction between a top and a  $b$ -quark and assuming  $|V_{td}|^2 + |V_{ts}|^2 \ll |V_{tb}|^2$ . The most general, lowest dimension,  $CP$  conserving (in effect of which couplings are real), Lagrangian for the  $Wtb$  vertex is given by [1–3]

$$\mathcal{L}_{Wtb} = \frac{g}{\sqrt{2}} \left[ W_\mu \bar{t} \gamma^\mu (V_{tb} f_1^L P_L + f_1^R P_R) b - \frac{1}{2m_W} W_{\mu\nu} \bar{t} \sigma^{\mu\nu} (f_2^L P_L + f_2^R P_R) b \right] + h.c. \quad (1.1)$$

where  $f_1^L \equiv 1 + \Delta f_1^L$ ,  $W_{\mu\nu} = D_\mu W_\nu - D_\nu W_\mu$ ,  $D_\mu = \partial_\mu - ieA_\mu$ ,  $P_{L,R} = \frac{1}{2}(1 \mp \gamma_5)$  are left- and right-handed projection operators,  $\sigma^{\mu\nu} = i/2(\gamma^\mu \gamma^\nu - \gamma^\nu \gamma^\mu)$  and  $g = e/\sin\theta_W$ . Since in the SM  $|V_{tb}| f_1^L \simeq 1$ , the  $\Delta f_1^L$  along other couplings  $f_2^L, f_1^R, f_2^R$  vanish at tree level, while there non-vanishing values are generated at the one loop level [4].  $Wtb$  anomalous couplings  $f_i$

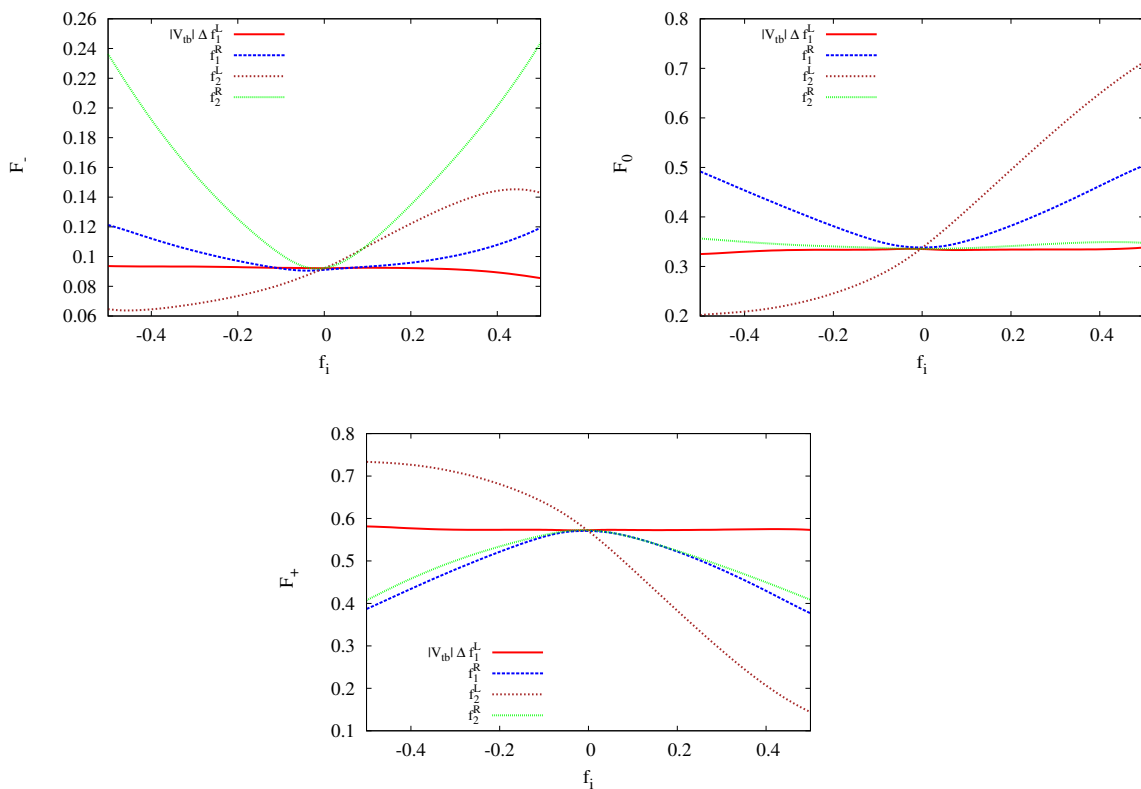


**Figure 4.** The variation of helicity fractions  $\mathcal{F}_-$ ,  $\mathcal{F}_0$  and  $\mathcal{F}_+$  as defined in the text with the anomalous coupling  $f_i$ .

are constrained from flavor physics. The magnitudes of the right-handed vector and tensor couplings can be indirectly constrained by the measured branching ratio of the  $b \rightarrow s\gamma$  process because they receive large contributions from loops involving the top quark and the  $W$ -boson. Current 95% C.L. bounds based on the CLEO data give  $|f_1^R| \leq 0.4 \times 10^{-2}$  at the  $2\text{-}\sigma$  level [5–7]. The branching ratio (BR)  $\text{BR}(b \rightarrow s\gamma)$  is computed by neglecting the terms proportional to the square of  $f_i$  in the matrix element squared. Assuming only one anomalous coupling to be non-zero at a time, the upper and lower limits for  $|V_{tb}| f_1^L, f_1^R, f_2^L$

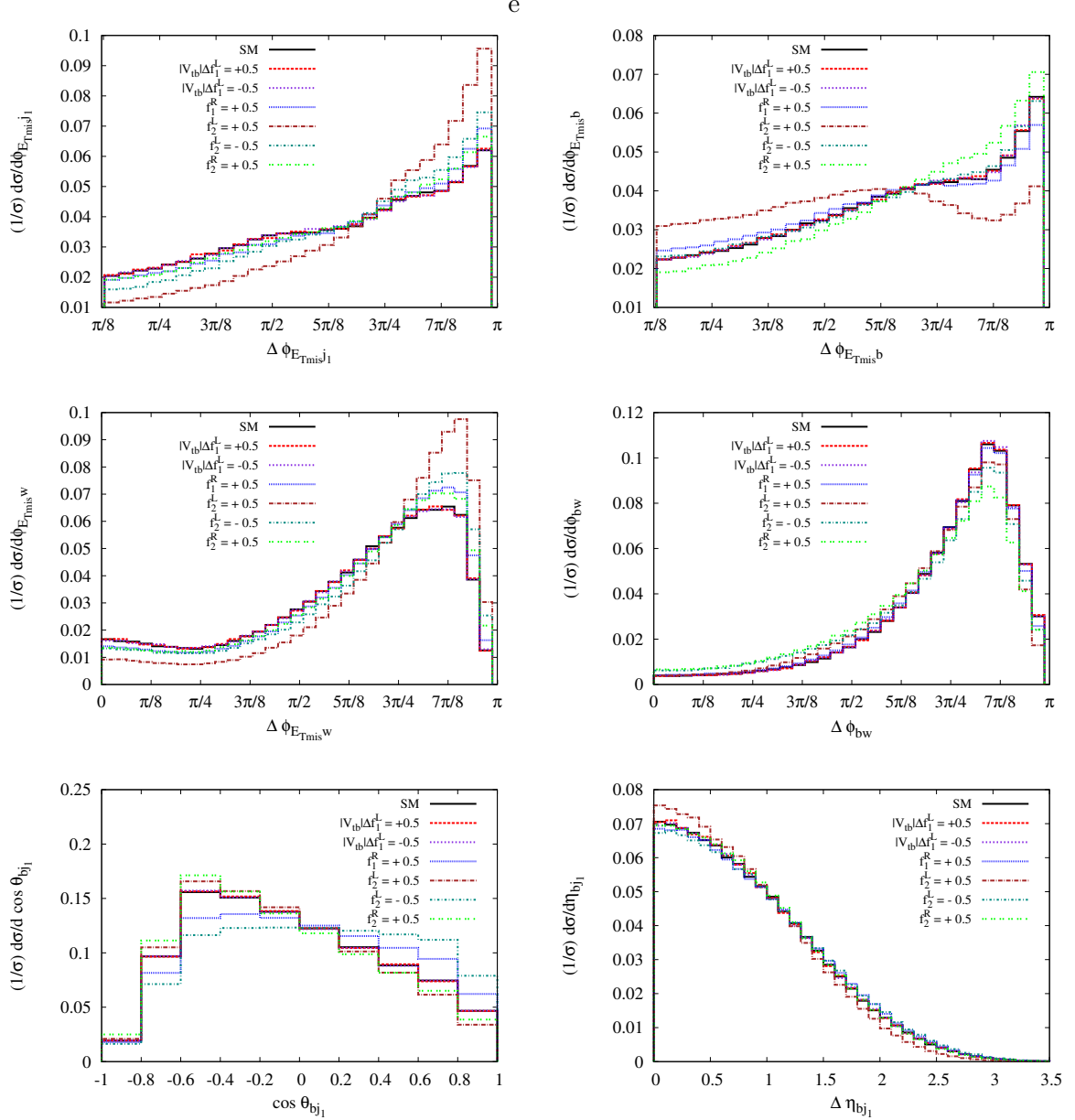


**Figure 5.** Normalized distributions of  $\Delta\phi_{\not{E}_T j_1}$ ,  $\Delta\phi_{\not{E}_T \bar{b}}$ ,  $\Delta\phi_{\not{E}_T W}$ ,  $\Delta\phi_{bW}$ ,  $\cos\theta_{\bar{b} j_1}$  and  $\Delta\eta_{\bar{b} j_1}$  for hadronic decay mode of  $W^-$ , corresponding to SM and an anomalous coupling of 0.5. Here  $j_1$  is the highest  $p_T$  jet.

and  $f_2^R$  obtained from the  $B$  decays are  $-0.13 \leq |V_{tb}| f_1^L \leq 0.03$ ,  $-0.0007 \leq f_1^R \leq 0.0025$ ,  $-0.0015 \leq f_2^L \leq 0.0004$  and  $-0.15 \leq f_2^R \leq 0.57$ , respectively [8]. If more than one couplings are taken non-zero simultaneously, their magnitudes in principle are not bound by  $b \rightarrow s\gamma$  alone and the limits can be very different.

The sensitivity of anomalous  $Wtb$  couplings can also be measured from  $W^\pm$  helicity distributions arising from top or antitop decays to their dominant  $Wb$  mode in the top-antitop pair production processes [9]. It can also be measured from the observed single

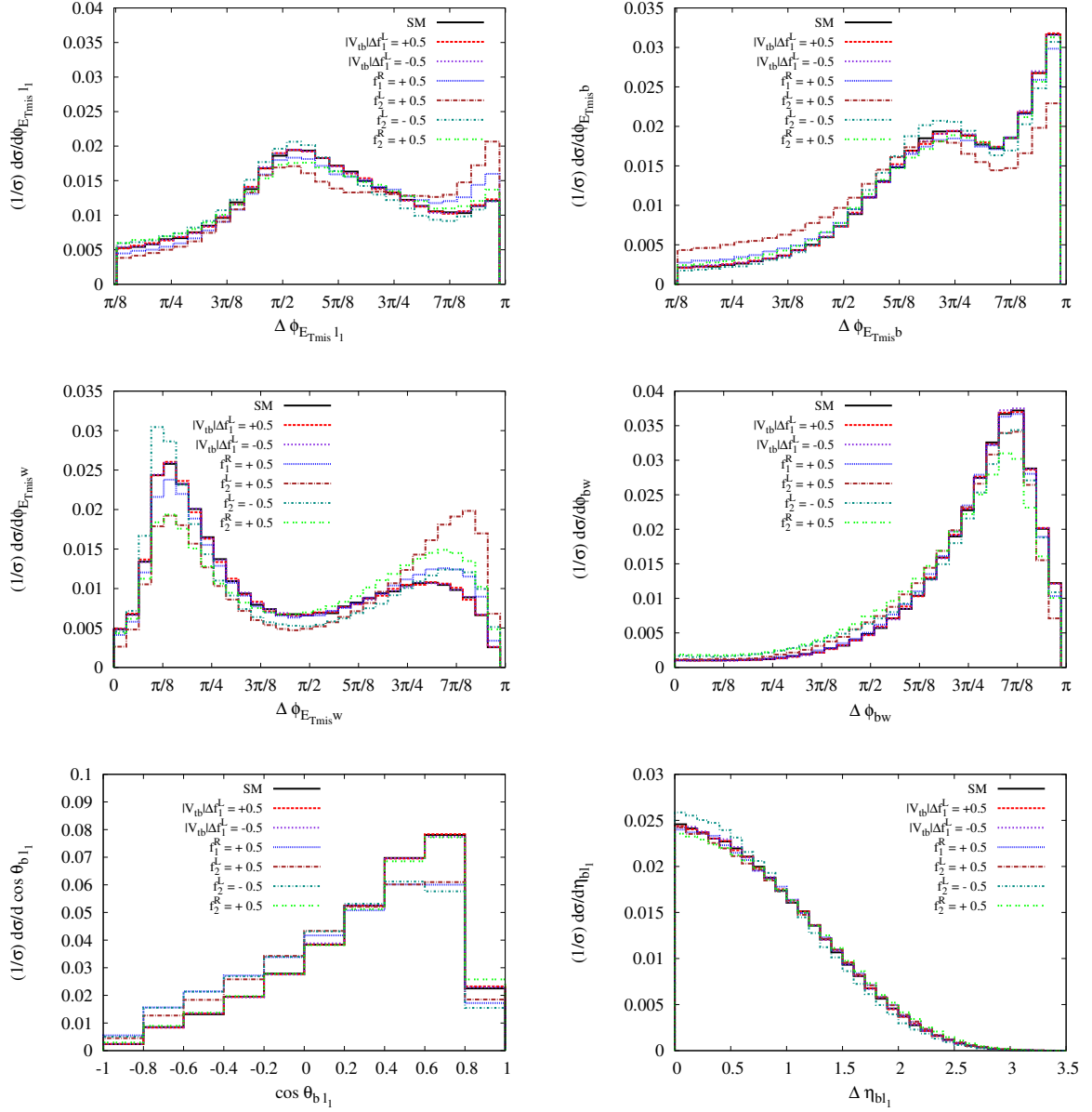


**Figure 6.** Normalized distributions of  $\Delta\phi_{\not{E}_T l_1}$ ,  $\Delta\phi_{\not{E}_T \bar{b}}$ ,  $\Delta\phi_{\not{E}_T W}$ ,  $\Delta\phi_{\bar{b} W}$ ,  $\cos\theta_{\bar{b} l_1}$  and  $\Delta\eta_{\bar{b} l_1}$  for leptonic decay mode of  $W^-$  corresponding to SM and an anomalous coupling of 0.5. Here  $l_1$  is the highest  $p_T$  charged lepton.

top or anti-top quark production cross section through  $W$ -boson exchange and has both the linear and quadratic terms in the effective couplings. Although the single top/ anti-top production in the SM is comparable (only a little less than half) to the  $t\bar{t}$  pair production, it is quite challenging to make the extraction due to considerable backgrounds at the Tevatron [10, 11] and the LHC [12, 13]. Recently DØ with  $5.4 \text{ fb}^{-1}$  data reported a combined analysis of  $W$  boson helicity studies and the single top quark production cross section exclusively through  $Wtb$  vertex *i.e.*  $|V_{td}|^2 + |V_{ts}|^2 \ll |V_{tb}|^2$ . This sets upper limits on anomalous  $Wtb$

couplings at 95 % C.L. assuming  $|V_{tb}| f_1^L = 1$  viz  $|f_2^L| \leq 0.224$ ,  $|f_1^R| \leq 0.548$ ,  $|f_2^R| \leq 0.347$  [14]. Sensitivity of the anomalous  $Wtb$  couplings on the cross-section of the associated  $tW$  production are also studied at LHC through  $\gamma p$  collision [15] and provide  $|f_2^L| \leq 0.22$ ,  $|f_1^R| \leq 0.55$ ,  $|f_2^R| \leq 0.35$ .

The sensitivity of the effective couplings in (1.1) corresponding to the different chiral vector and tensor current can be studied through one-dimensional distributions of kinematic observables. These distributions manifest a certain amount of associated asymmetry depending on the specific Lorentz structure, which can then be used as a discriminator to constraint these anomalous couplings. Based on associated asymmetries generated from the measured angular distributions of  $\cos\theta^{*1}$  defined in [16], the ATLAS collaboration [17] set limits on single anomalous couplings at 95% C.L. to be  $\text{Re}(f_1^R) \in [-0.44, 0.48]$ ,  $\text{Re}(f_2^L) \in [-0.24, 0.21]$  and  $\text{Re}(f_2^R) \in [-0.49, 0.15]$ . Constraints on  $Wtb$  vertex based on the angular asymmetries constructed from ATLAS data and the t-channel single top cross section in CMS have been analysed in [18].

Effects of anomalous coupling on angular distributions of  $b$ -quark and  $\mu^+$  have been studied in  $e^+e^-$  linear collider with one specific semileptonic channel in the double resonance approximation for the  $t$  and  $\bar{t}$  production [19–22]. A preliminary study of the sensitivity of  $Wtb$  anomalous couplings on the single top quark production cross-section in  $e^-p$  collision for TESLA+HERA and LHC+CLIC energies has been performed in [23].

Recently a deep inelastic electron-nucleon scattering facility is proposed at the LHC, known as LHeC. It is proposed that an electron beam of 60 GeV will collide with 7 TeV proton beam simultaneous to the existing proton-proton collision experiments at the LHC [24–26]. The LHeC is expected to test the rich electroweak physics with precision. There has been some work on the physics goals of the collider [24–29]. The working group involved in the synergy between LHC and LHeC brought out an excellent report showing the interdependencies of the physics reach and goals of both these colliders [30]. LHeC is going to provide an unprecedented platform for studying the single top quark production as this has an advantage over the LHC and the TeVatron in terms of providing (a) a clean environment with suppressed background from strong interaction initiated processes, and (b) a kinematic reach for lepton-nucleon scattering at c.m. energy around 1.3 TeV. Thus it is worthwhile to study the single top quark production and probe the  $Wtb$  anomalous couplings at the LHeC.

In Sec. 2 we analyze and study the single anti-top quark production, its yield, choice of selection cuts and kinematic distributions at LHeC. We introduce kinematic asymmetries as estimators in Sec. 3, provide the exclusion contours based on  $\chi^2$  analysis and using the method of optimal variables give error correlation matrices. Finally the summary of our observations is given in Sec. 4.

Event Selection	SM	$f_1^R = .5$	$f_2^L = .5$	$f_2^L = -.5$	$f_2^R = .5$	$ V_{tb}  \Delta f_1^L = .5$
No Selection cuts	$1.11 \times 10^5$ $\pm 3.3 \times 10^2$	$1.81 \times 10^5$ $\pm 4.3 \times 10^2$	$6.44 \times 10^4$ $\pm 2.5 \times 10^2$	$2.77 \times 10^5$ $\pm 5.3 \times 10^2$	$2.59 \times 10^5$ $\pm 5.1 \times 10^2$	$5.66 \times 10^5$ $\pm 7.5 \times 10^2$
$p_{T_{j,\bar{b}}} \geq 20$ GeV	$7.78 \times 10^4$ $\pm 2.8 \times 10^2$	$1.28 \times 10^5$ $\pm 3.6 \times 10^2$	$4.75 \times 10^4$ $\pm 2.2 \times 10^2$	$1.81 \times 10^5$ $\pm 4.3 \times 10^2$	$1.76 \times 10^5$ $\pm 4.2 \times 10^2$	$3.93 \times 10^5$ $\pm 6.3 \times 10^2$
$p_{T_{j,\bar{b}}} \geq 20$ GeV $\cancel{E}_T \geq 25$ GeV	$5.74 \times 10^4$ $\pm 2.4 \times 10^2$	$9.57 \times 10^4$ $\pm 3.1 \times 10^2$	$3.81 \times 10^4$ $\pm 1.9 \times 10^2$	$1.37 \times 10^5$ $\pm 3.7 \times 10^2$	$1.42 \times 10^5$ $\pm 3.8 \times 10^2$	$2.90 \times 10^5$ $\pm 5.4 \times 10^2$
$p_{T_{j,\bar{b}}} \geq 20$ GeV $\cancel{E}_T \geq 25$ GeV $ \eta_j  < 5,  \eta_{\bar{b}}  < 2.5$	$4.75 \times 10^4$ $\pm 2.2 \times 10^2$	$8.21 \times 10^4$ $\pm 2.9 \times 10^2$	$3.05 \times 10^4$ $\pm 1.8 \times 10^2$	$1.16 \times 10^5$ $\pm 3.4 \times 10^2$	$1.22 \times 10^5$ $\pm 3.5 \times 10^2$	$2.40 \times 10^5$ $\pm 4.9 \times 10^2$
$p_{T_{j,\bar{b}}} \geq 20$ GeV $\cancel{E}_T \geq 25$ GeV $ \eta_j  < 5,  \eta_{\bar{b}}  < 2.5$ $\Delta\phi_{j\cancel{E},\bar{b}\cancel{E}} > 0.4$	$3.67 \times 10^4$ $\pm 1.9 \times 10^2$	$6.41 \times 10^4$ $\pm 2.5 \times 10^2$	$2.43 \times 10^4$ $\pm 1.6 \times 10^2$	$9.20 \times 10^4$ $\pm 3.0 \times 10^2$	$9.71 \times 10^4$ $\pm 3.1 \times 10^2$	$1.86 \times 10^5$ $\pm 4.3 \times 10^2$
$p_{T_{j,\bar{b}}} \geq 20$ GeV $\cancel{E}_T \geq 25$ GeV $ \eta_j  < 5,  \eta_{\bar{b}}  < 2.5$ $\Delta\phi_{j\cancel{E},\bar{b}\cancel{E}} > 0.4$ $\Delta R_{jj,j\bar{b}} > 0.4$	$3.65 \times 10^4$ $\pm 1.9 \times 10^2$	$6.37 \times 10^4$ $\pm 2.5 \times 10^2$	$2.43 \times 10^4$ $\pm 1.5 \times 10^2$	$9.11 \times 10^4$ $\pm 3.0 \times 10^2$	$9.58 \times 10^4$ $\pm 3.1 \times 10^2$	$1.85 \times 10^5$ $\pm 4.3 \times 10^2$
Fiducial Efficiency	32.73 %	35.19 %	37.74 %	32.90 %	37.07 %	32.75 %

**Table 1.** Yields  $N \pm \sqrt{N}$  without/ with selection cuts in the hadronic channel corresponding to the chosen anomalous coupling value of 0.5 at integrated luminosity  $L = 100 \text{ fb}^{-1}$ .

## 2 Single anti-top quark production

In hadron colliders, the SM single top quark production at leading order is studied through three disparate non-interfering modes via  $s$ -,  $t$ - and  $Wt$ - channels, respectively and details can be found in [31]. The  $t$ - channel through charge current (CC) interactions dominates over all the other production mechanisms. In the LHeC we can study the single top quark production only through the  $t$  channel process  $e^- \bar{b} \rightarrow \nu_e \bar{t} + X$  as shown in Figure 1. In sharp contrast to the LHC the absence of pile-up and underlying event effects at LHeC, high rates of single anti-top production is expected to provide a better insight on  $Wtb$  anomalous couplings. The sensitivity of the  $Wtb$  couplings are also investigated through the sub-dominant associated  $tW$  production in references [32, 33].

We have implemented  $Wtb$  effective couplings corresponding to both chiral vector and tensor structures given by the Lagrangian (1.1) in MadGraph/MadEvent [34] using FeynRules [35]. The partonic cross sections are convoluted with CTEQ6L1 parton distribution functions (PDF) keeping factorization and renormalization scale  $\mu_F = \mu_R = m_t = 172.5$

<sup>1</sup>The cosine of the angle  $\theta^*$  between the momentum direction of the charged lepton from the W-boson decay and the reversed momentum direction of the b quark from top-quark decay, both boosted into the W-boson rest frame.



GeV. The mass of  $b$ -quark  $m_b = 4.7$  GeV and  $W^\pm$  boson  $m_W = 79.83$  GeV, assuming the SM value for  $|V_{tb}| f_1^L = 1$ . We study the process  $e^- \bar{b} \rightarrow \nu_e \bar{t} + X$  and probe the accuracy with which the anomalous couplings can be measured. The variation of the cross-section of the single top production in SM is studied with respect to the center of mass energy and electron energy in Figure 2 and we are in agreement with the earlier results given in [23]. We also show the effect of taking 60% and 80 % beam polarizations, which results in the enhancement of the SM single top production cross section.

The new physics effect can arise either at the production vertex of the anti-top in the process  $e^- p \rightarrow \bar{t} \nu_e \rightarrow \bar{b} W^- \nu_e$  or at the decay vertex. The feynman diagram with anomalous couplings at both the vertices is highly suppressed. Figure 3 depicts the interplay of the interference terms and shows the variation of the cross section with respect to the variation in the anomalous couplings. We estimate and study the  $W^-$  helicity distributions arising from NP effects. As mentioned earlier, the  $W$  polarization distribution can be a sensitive observable to distinguish the contribution of anomalous couplings. We study the behavior of the helicity fractions of the  $W^-$  in terms of ratios of the number of events  $\mathcal{F}_- = N_-/N$ ,  $\mathcal{F}_+ = N_+/N$  and  $\mathcal{F}_0 = N_0/N$  where  $N_-$ ,  $N_+$  and  $N_0$  are the left, right and longitudinally polarized  $W^-$  events and  $N = N_+ + N_- + N_0$ . We vary the coupling and study its effect through the variation on these ratios in Figure 4. These curves are drawn for the choice  $E_e^- = 60$  GeV and  $E_p = 7$  TeV with an integrated luminosity  $L = 100 \text{ fb}^{-1}$ . We observe that

- (a) The  $\mathcal{F}_-$  and  $\mathcal{F}_+$  corresponding to the positive and negative polarized  $W$ 's show opposite trend with the variation of couplings.
- (b)  $\mathcal{F}_-$  is highly sensitive to the right handed tensor current as it has a larger momentum dependence in comparison to the right handed vector chiral current.
- (c) The contribution of longitudinally polarized  $W$  bosons grows with the increase in the couplings corresponding to the left handed tensor and right handed vector currents.

Finally we analyze the anti-top through the hadronic and leptonic decay modes of  $W$ 's. We fix electron energy  $E_e = 60$  GeV and proton  $E_p = 7$  TeV throughout the analysis as per recommendations given in the LHeC technical design report [24].

## 2.1 Sensitivity in the Hadronic Mode

In order to study the sensitivity of the anomalous couplings introduced in 1.1, we first examine the process  $e^- p \rightarrow \bar{t} \nu_e, (\bar{t} \rightarrow W^- \bar{b}, W^- \rightarrow jj), j \equiv \bar{u}, d, \bar{c}, s$  at LHeC and the potential backgrounds. We then apply appropriate selection cuts to considerably reduce the background. As mentioned earlier, unlike hadronic colliders the sensitivity in this mode is expected to be better due to less severe hadronic backgrounds.

- (a) The process  $e^- p \rightarrow \nu_e W^- \bar{b}$  wherein the  $W^- \bar{b}$  is generated from with and without anti-top quarks is analyzed. The cross-section is found to be dominated by diagrams with the anti-top. The cross-section of diagrams without anti-top is just about 1% of the cross-section with anti-top lines.

- (b) The processes with  $e^-p \rightarrow \nu_e j \mathcal{J} \mathcal{J}$  with ( $\mathcal{J} \equiv u, \bar{u}, d, \bar{d}, s, \bar{s}, b, \bar{b}, g$ ), where light  $u, d, s, \bar{u}, \bar{d}, \bar{s}$  and  $c, \bar{c}$  partons have a probability of  $\sim 1/100$  and  $1/10$  respectively to fake the  $b$  or  $\bar{b}$  quarks are studied. The imposition of  $p_T \geq 20$  GeV can reduce this background to  $\sim 4.7$  pb without compromising much on the signal cross-section.
- (c) The potential background to the above process arises from the diagrams leading to  $e^-p \rightarrow \nu_e j b \bar{b}$ . We find that the cross-section with a  $p_T$  cut on partons,  $p_T \geq 20$  GeV, reduces this to  $\sim 50$  fb, thus rendering this to a quasi-irreducible negligible background.

Event Selection	SM	$f_1^R = .5$	$f_2^L = .5$	$f_2^L = -.5$	$f_2^R = .5$	$ V_{tb}  \Delta f_1^L = .5$
No selection cuts	$3.72 \times 10^4$ $\pm 1.9 \times 10^2$	$6.03 \times 10^4$ $\pm 2.5 \times 10^2$	$2.14 \times 10^4$ $\pm 1.5 \times 10^2$	$9.23 \times 10^4$ $\pm 3.0 \times 10^2$	$8.61 \times 10^4$ $\pm 2.9 \times 10^2$	$1.88 \times 10^5$ $\pm 4.3 \times 10^2$
$p_{T_{j,\bar{b}}} \geq 20$ GeV	$2.46 \times 10^4$ $\pm 1.6 \times 10^2$	$4.21 \times 10^4$ $\pm 2.1 \times 10^2$	$1.60 \times 10^4$ $\pm 1.3 \times 10^2$	$5.33 \times 10^4$ $\pm 2.3 \times 10^2$	$6.13 \times 10^4$ $\pm 2.5 \times 10^2$	$1.24 \times 10^5$ $\pm 2.5 \times 10^2$
$p_{T_{j,\bar{b}}} \geq 20$ GeV $\cancel{E}_T \geq 25$ GeV	$1.47 \times 10^4$ $\pm 1.2 \times 10^2$	$2.49 \times 10^4$ $\pm 1.6 \times 10^2$	$1.02 \times 10^4$ $\pm 1.0 \times 10^2$	$3.41 \times 10^4$ $\pm 1.9 \times 10^2$	$3.63 \times 10^4$ $\pm 1.9 \times 10^2$	$7.46 \times 10^4$ $\pm 2.7 \times 10^2$
$p_{T_{j,\bar{b}}} \geq 20$ GeV $\cancel{E}_T \geq 25$ GeV $ \eta_j  < 5,  \eta_{\bar{b}}  < 2.5$	$1.18 \times 10^4$ $\pm 1.1 \times 10^2$	$2.02 \times 10^4$ $\pm 1.4 \times 10^2$	$7.96 \times 10^3$ $\pm 8.9 \times 10^1$	$2.55 \times 10^4$ $\pm 1.6 \times 10^2$	$3.04 \times 10^4$ $\pm 1.7 \times 10^2$	$6.0 \times 10^4$ $\pm 2.4 \times 10^2$
$p_{T_{j,\bar{b}}} \geq 20$ GeV $\cancel{E}_T \geq 25$ GeV $ \eta_j  < 5,  \eta_{\bar{b}}  < 2.5$ $\Delta\phi_{j\cancel{E},\bar{b}\cancel{E}} > 0.4$	$9.37 \times 10^3$ $\pm 9.7 \times 10^1$	$1.6 \times 10^4$ $\pm 1.2 \times 10^2$	$6.12 \times 10^3$ $\pm 7.8 \times 10^1$	$2.04 \times 10^4$ $\pm 1.43 \times 10^2$	$2.34 \times 10^4$ $\pm 1.5 \times 10^2$	$4.74 \times 10^4$ $\pm 2.2 \times 10^2$
$p_{T_{j,\bar{b}}} \geq 20$ GeV $\cancel{E}_T \geq 25$ GeV $ \eta_j  < 5,  \eta_{\bar{b}}  < 2.5$ $\Delta\phi_{j\cancel{E},\bar{b}\cancel{E}} > 0.4$ $\Delta R_{jj,\bar{b}\bar{b}} > 0.4$	$9.34 \times 10^3$ $\pm 9.7 \times 10^1$	$1.59 \times 10^4$ $\pm 1.2 \times 10^2$	$6.12 \times 10^3$ $\pm 7.8 \times 10^1$	$2.02 \times 10^4$ $\pm 1.4 \times 10^2$	$2.33 \times 10^4$ $\pm 1.5 \times 10^2$	$4.72 \times 10^4$ $\pm 2.2 \times 10^2$
Fiducial Efficiency	25.08 %	26.42 %	28.50 %	21.93 %	27.04 %	25.07 %

**Table 2.** Yields  $N \pm \sqrt{N}$  without/ with selection cuts in the leptonic channel corresponding to the chosen anomalous coupling value of 0.5 at integrated luminosity  $L = 100 \text{ fb}^{-1}$ .

To reduce the background following selection cuts are adopted :-

- (i) Minimum of transverse momentum of jets, leptons and  $\bar{b}$ -antiquark to be  $p_{T_{j,\bar{b}}} > 20$  GeV.
- (ii) Missing transverse energy taken to be  $\cancel{E}_T > 25$  GeV.
- (iii) The pseudo-rapidity region for leptons and  $\bar{b}$ -antiquark is taken to be  $|\eta_{\bar{b},l}| < 2.5$ , however for jets  $|\eta_j| < 5$ .
- (iv) The difference of azimuthal angle between missing energy  $\cancel{E}_T$  and jets, leptons,  $\bar{b}$ -antiquark should be  $\Delta\phi > 0.4$ .

- (v) Imposing isolation cuts for lighter, heavy quarks and lepton require  $\Delta R_{ij} > 0.4$  where  $i, j \equiv$  leptons, jets and  $\bar{b}$  anti-quarks.

To probe the effect of these cuts on the yield, we study the effect of these cuts on the SM and at the effective coupling representative value of 0.5. The analysis is summarized in Table 1 and the overall fiducial efficiencies are presented.

The characteristics of the highest  $p_T$  jet  $j_1$ , the final state  $\bar{b}$  are likely to bear the signature of the  $Wtb$  couplings at the decay vertex. We study one dimensional distributions of azimuthal angle (angle between the planes)  $\Delta\phi_{\cancel{E}_T, j_1}$ ,  $\Delta\phi_{\cancel{E}_T, \bar{b}}$ ,  $\Delta\phi_{\cancel{E}_T, W}$  and  $\Delta\phi_{\bar{b}, W}$  along with the  $\cos\theta_{\bar{b}j_1}$  and  $\Delta\eta_{\bar{b}j_1}$ . Figure 5 exhibit these distributions. All histograms are normalized to unity and are drawn for a anomalous coupling representative value 0.5. The anomalous coupling  $f_1^R$  shows a discriminating behavior for the differential distribution  $d\sigma/d\cos\theta_{\bar{b}j_1}$ , while  $f_2^R$  uniquely shows a different profile in most of the distribution given in Figure 5. Since the positive  $f_2^L$  interferes constructively with SM and has a large momentum dependence it not only enhances the contribution but also changes the distribution profile of SM.

## 2.2 Sensitivity in the Leptonic Mode

Similarly we study the yield of the leptonic decay mode of  $W^-$  through the process  $e^-p \rightarrow \bar{t}\nu_e$ , ( $\bar{t} \rightarrow W^-\bar{b}$ ,  $W^- \rightarrow l^-\bar{\nu}_l$ ),  $l^- \equiv e^-, \mu^-$  at LHeC. Here we do not have any large background. The standard selection cuts are same as those given in 2.1. The fiducial efficiencies with representative value 0.5 corresponding to the coefficient of the different chiral and Lorentz structures as given in (1.1) are shown in Table 2.

In the leptonic mode the final state charged lepton along with  $\bar{b}$  shows the characteristic features of the anomalous couplings. Further we study the sensitivity of the couplings through one dimensional distributions corresponding to azimuthal angle  $\Delta\phi_{\cancel{E}_T, l_1}$ ,  $\Delta\phi_{\cancel{E}_T, \bar{b}}$ ,  $\Delta\phi_{\cancel{E}_T, W^-}$  and  $\Delta\phi_{\bar{b}, W^-}$  along with the polar angle  $\cos\theta_{\bar{b}l_1}$  and difference of pseudo-rapidity  $\Delta\eta_{\bar{b}l_1}$  between  $\bar{b}$  and the charged lepton with highest  $p_T$  designated as  $l_1$ . Figure 6 depict these distributions.

- (a) Positive value of  $|V_{tb}|\Delta f_1^L$  provides the SM like distribution, while its negative value interferes destructively decreasing the cross-section to zero at  $|V_{tb}|\Delta f_1^L = -1$ .
- (b)  $f_2^L > 0$  ( $f_2^L < 0$ ) enhances (suppresses) the SM profile in all distributions due to constructive (destructive) interferences with SM.
- (c) The right-handed vector and tensor couplings  $f_1^R$  and  $f_2^R$  do not interfere with the SM terms therefore, their sensitivity is less in comparison to the terms arising from the left-handed couplings and this is evident from the distributions shown in Figure 6.

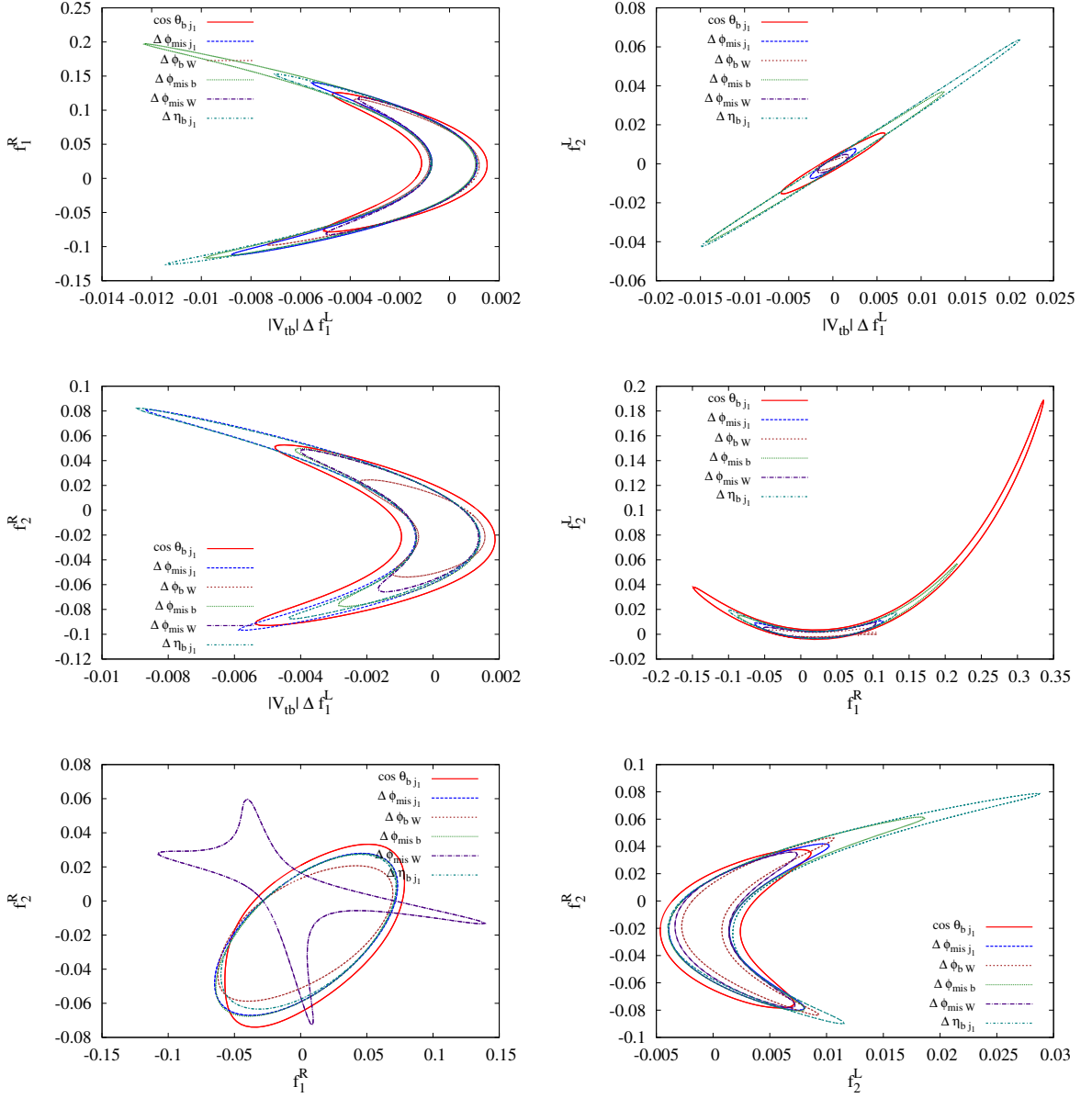


**Figure 7.** 68.3 % C.L. exclusion contours on the plane of  $|V_{tb}| \Delta f_1^L - f_1^R$ ,  $|V_{tb}| \Delta f_1^L - f_2^L$ ,  $|V_{tb}| \Delta f_1^L - f_2^R$ ,  $f_1^R - f_2^L$ ,  $f_1^R - f_2^R$  and  $f_2^L - f_2^R$  based on bin analysis for all kinematic observables in the hadronic decay mode of  $W^-$ .

### 3 Estimators and $\chi^2$ analysis

#### 3.1 Angular Asymmetries from Histograms

We construct the asymmetry from the distribution of kinematic observables in both the hadronic and leptonic modes. These asymmetries can be sensitive discriminators to distinguish the contribution from the different Lorentz structure due to their characteristic momentum dependence. We study the angular asymmetries *w.r.t* the polar angle  $\cos \theta_{ij}$ ,

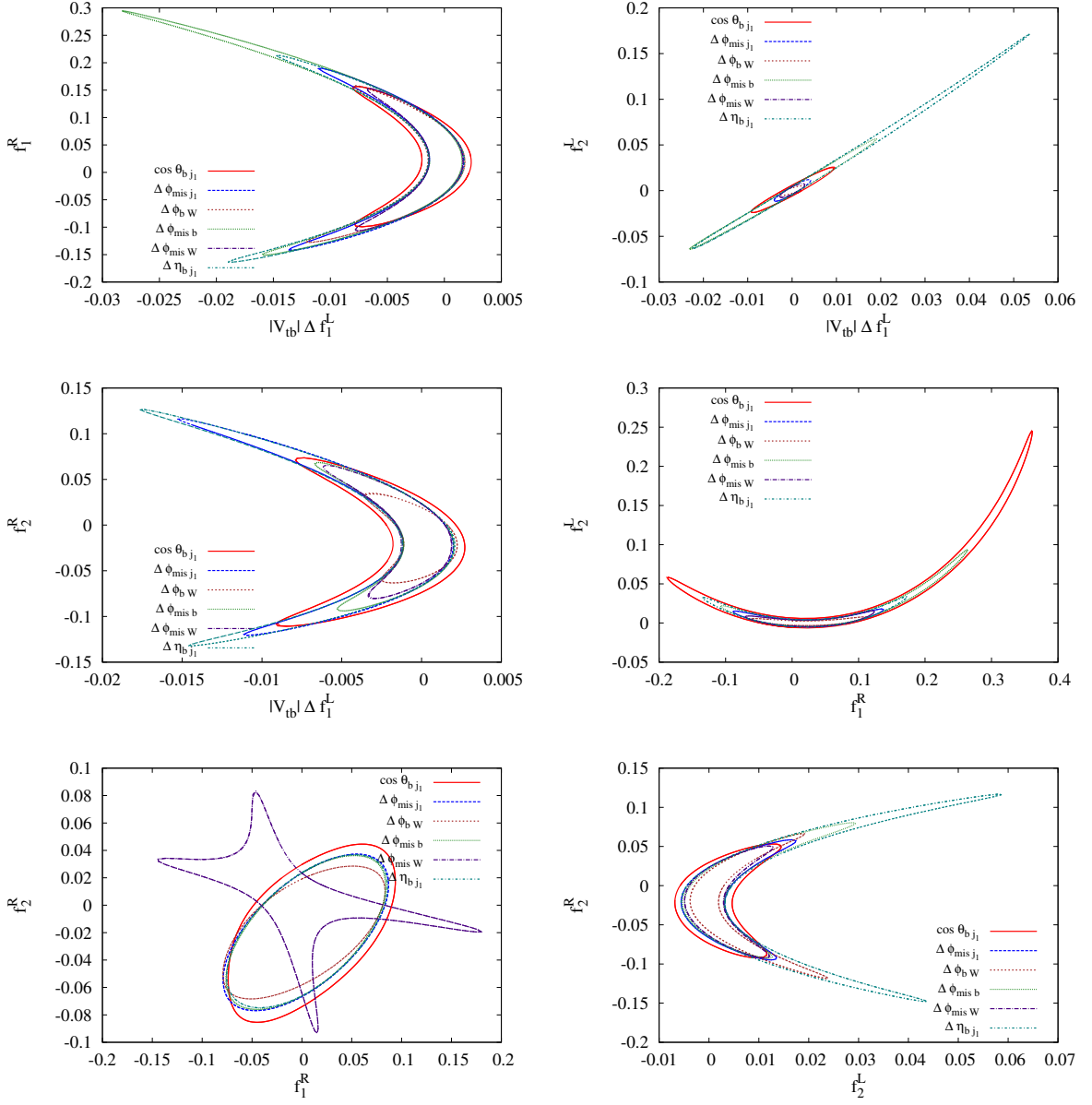


**Figure 8.** 95 % C.L. exclusion contours on the plane of  $|V_{tb}| \Delta f_1^L - f_1^R$ ,  $|V_{tb}| \Delta f_1^L - f_2^L$ ,  $|V_{tb}| \Delta f_1^L - f_2^R$ ,  $f_1^R - f_2^L$ ,  $f_1^R - f_2^R$  and  $f_2^L - f_2^R$  based on bin analysis for all kinematic observables in the hadronic decay mode of  $W^-$ .

rapidity difference  $\Delta \eta_{ij}$  and azimuthal angle difference  $\Delta \phi_{ij}$ , where  $i, j$  may be any partons (including  $\bar{b}$ -antiquark), charged lepton or missing energy to the respective planes. The

associated asymmetries  $A_{\theta_{ij}}$ ,  $A_{\Delta\eta_{ij}}$  and  $A_{\Delta\Phi_{ij}}$  are defined as

$$A_{\theta_{ij}} = \frac{N_+^A(\cos\theta_{ij} > 0) - N_-^A(\cos\theta_{ij} < 0)}{N_+^A(\cos\theta_{ij} > 0) + N_-^A(\cos\theta_{ij} < 0)} \quad (3.1)$$

$$A_{\Delta\eta_{ij}} = \frac{N_+^A(\Delta\eta_{ij} > 0) - N_-^A(\Delta\eta_{ij} < 0)}{N_+^A(\Delta\eta_{ij} > 0) + N_-^A(\Delta\eta_{ij} < 0)} \quad (3.2)$$

$$A_{\Delta\Phi_{ij}} = \frac{N_+^A(\Delta\phi_{ij} > \frac{\pi}{2}) - N_-^A(\Delta\phi_{ij} < \frac{\pi}{2})}{N_+^A(\Delta\phi_{ij} > \frac{\pi}{2}) + N_-^A(\Delta\phi_{ij} < \frac{\pi}{2})} \quad (3.3)$$

with  $0 \leq \Delta\phi_{ij} \leq \pi$ . In order to calculate the asymmetry  $A_\alpha$  and its statistical error for  $N_+^A$  and  $N_-^A$  events with  $N = (N_+^A + N_-^A) = L \cdot \sigma$ , we use the following definition based on binomial distribution :

$$A_\alpha = a \pm \sigma_a, \quad \text{where} \quad (3.4)$$

$$a = \frac{N_+^A - N_-^A}{N_+^A + N_-^A} \quad \text{and} \quad \sigma_a = \sqrt{\frac{1 - a^2}{L \cdot \sigma}}; \quad (\alpha = \cos\theta_{ij}, \Delta\eta_{ij}, \Delta\Phi_{ij}) \quad (3.5)$$

Based on the one dimensional histograms given in Figures 5 and 6, we look for the asymmetry within a distribution generated due to the interplay of the SM and a given anomalous coupling for two distinct modes of  $W^-$  decay. On comparing with SM asymmetry any large deviation from it would imply that the associated kinematic observable is an optimal variable in determining the sensitivity of the given anomalous coupling. We provide these asymmetries constructed from the distributions in Table 3 and 4 for a representative value of the coupling 0.5. We do not construct any asymmetry with respect to distributions corresponding to  $\Delta f_1^L$  as they will be identically same as SM. It can be easily read out

	$A_{\Delta\Phi_{\not{E}_T j_1}}$	$A_{\Delta\Phi_{\not{E}_T \bar{b}}}$	$A_{\Delta\Phi_{\not{E}_T W^-}}$	$A_{\Delta\Phi_{W^- \bar{b}}}$	$A_{\theta_{\bar{b} j_1}}$	$A_{\Delta\eta_{b j_1}}$
SM	.386 ± .005	.380 ± .005	.469 ± .005	.779 ± .003	-.123 ± .005	-.037 ± .005
$f_1^R = +.5$	.433 ± .004	.338 ± .004	.531 ± .003	.760 ± .003	.003 ± .004	.071 ± .004
$f_2^L = -.5$	.493 ± .003	.378 ± .003	.558 ± .003	.655 ± .003	.101 ± .003	.163 ± .003
$f_2^L = +.5$	.613 ± .005	.197 ± .006	.689 ± .005	.725 ± .004	-.191 ± .006	-.269 ± .006
$f_2^R = +.5$	.431 ± .003	.462 ± .003	.529 ± .003	.632 ± .003	-.198 ± .003	-.114 ± .003

**Table 3.** Asymmetries and its error associated with the kinematic distributions in Figure 5 at an integrated luminosity  $L = 100 \text{ fb}^{-1}$ . These asymmetries are computed for a representative value of the anomalous coupling 0.5 along with SM.

from the Tables 3 and 4 that unlike  $f_1^R$  and  $f_2^R$ ,  $f_2^L$  is sensitive to all asymmetries in both hadronic and leptonic modes.

Asymmetries shown in the figures of merit 3 and 4 are good estimators for preliminary studies. They give a handle for judging the ability of the measured observable to distinguish the contribution from an anomalous term in the Lagrangian. But they may not be sensitive enough for the couplings which are one order of magnitude smaller than the representative value. In fact the whole distribution is essentially divided into two halves which corresponds to only two bins with large bin-width. The asymmetries induced by the tiny new physics couplings among these two large bins is likely to vanish.

	$A_{\Delta\Phi_{\tilde{E}_T l_1}}$	$A_{\Delta\Phi_{\tilde{E}_T \bar{b}}}$	$A_{\Delta\Phi_{\tilde{E}_T W^-}}$	$A_{\Delta\Phi_{W^- \bar{b}}}$	$A_{\theta_{\tilde{b} l_1}}$	$A_{\Delta\eta_{\tilde{b} l_1}}$
SM	$.334 \pm .010$	$.749 \pm .007$	$-.216 \pm .010$	$.827 \pm .006$	$-.570 \pm .009$	$-.312 \pm .010$
$f_1^R = +.5$	$.391 \pm .007$	$.698 \pm .006$	$-.131 \pm .008$	$.817 \pm .005$	$-.379 \pm .007$	$-.129 \pm .008$
$f_2^L = -.5$	$.282 \pm .007$	$.766 \pm .005$	$-.182 \pm .007$	$.730 \pm .005$	$-.383 \pm .007$	$-.021 \pm .007$
$f_2^L = +.5$	$.412 \pm .012$	$.569 \pm .011$	$.082 \pm .013$	$.771 \pm .008$	$-.421 \pm .012$	$-.320 \pm .012$
$f_2^R = +.5$	$.327 \pm .006$	$.715 \pm .005$	$.005 \pm .007$	$.707 \pm .005$	$-.562 \pm .005$	$-.337 \pm .006$

**Table 4.** Asymmetries and its error associated with the kinematic distributions in Figure 6 at an integrated luminosity  $L = 100 \text{ fb}^{-1}$ . These asymmetries are computed for a representative value of the anomalous coupling 0.5 along with SM.

### 3.2 Exclusion contours from bin analysis

In this subsection the sensitivity of couplings are obtained through  $\chi^2$  analysis, where we compute the sum of the variance of events over all bins. Thus with more bin information we expect to achieve a better sensitivity than the asymmetries which is generated essentially by dividing the whole distribution into two equal bins only.

To make the analysis more effective we switch on two effective anomalous couplings at a time with SM. The  $\chi^2$  becomes a function of two effective anomalous couplings  $f_i, f_j$  and defined as

$$\chi^2(f_i, f_j) = \sum_{k=1}^N \left( \frac{\mathcal{N}_k^{\text{exp}} - \mathcal{N}_k^{\text{th}}(f_i, f_j)}{\delta \mathcal{N}_k^{\text{exp}}} \right)^2 \quad (3.6)$$

where  $\mathcal{N}_k^{\text{th}}(f_i, f_j)$  and  $\mathcal{N}_k^{\text{exp}}$  are the total number of events predicted by the theory involving  $f_i, f_j$  and measured in the experiment for the  $k^{\text{th}}$  bin respectively.  $\delta \mathcal{N}_k^{\text{exp}}$  is the combined statistical and systematic error  $\delta_{\text{sys}}$  in measuring the events for the  $k^{\text{th}}$  bin. If all the coefficients  $f_i$ 's are small, then the experimental result in the  $k^{\text{th}}$  bin should be approximated by the SM prediction as

$$\mathcal{N}_k^{\text{exp}} \approx \mathcal{N}_k^{\text{SM}}. \quad (3.7)$$

The error  $\delta \mathcal{N}_k^{\text{SM}}$  can be defined as

$$\delta \mathcal{N}_k^{\text{SM}} = \sqrt{\mathcal{N}_k^{\text{SM}} (1 + \delta_{\text{sys}})}. \quad (3.8)$$

We consider 2% systematic error for our analysis.

The analysis is performed for both hadronic and leptonic observables which depends on the distributions shown in Figures 5 and 6. Using this definition of  $\chi^2$  in (3.6), we draw the 68.3% and 95% C.L. exclusion contours on the six different two dimensional planes defined by the anomalous couplings  $|V_{tb}| \Delta f_1^L, f_1^R, f_2^L$  and  $f_2^R$ . 68.3% and 95% C.L. exclusion contours for the hadronic channel are shown in Figures 7 and 8 respectively. Similarly 68.3% and 95% C.L. exclusion contours for the leptonic channel are shown in Figures 9 and 10 respectively.

Examining the 68.3 % C.L. exclusion contours in hadronic and leptonic modes, we find that  $|V_{tb}| \Delta f_1^L$  and  $f_2^L$  exhibits the sensitivity at the  $\mathcal{O} \sim 10^{-3}$ , while the coefficients of the right handed vector and tensor current are sensitive at the best  $\mathcal{O} \sim 10^{-2}$ .

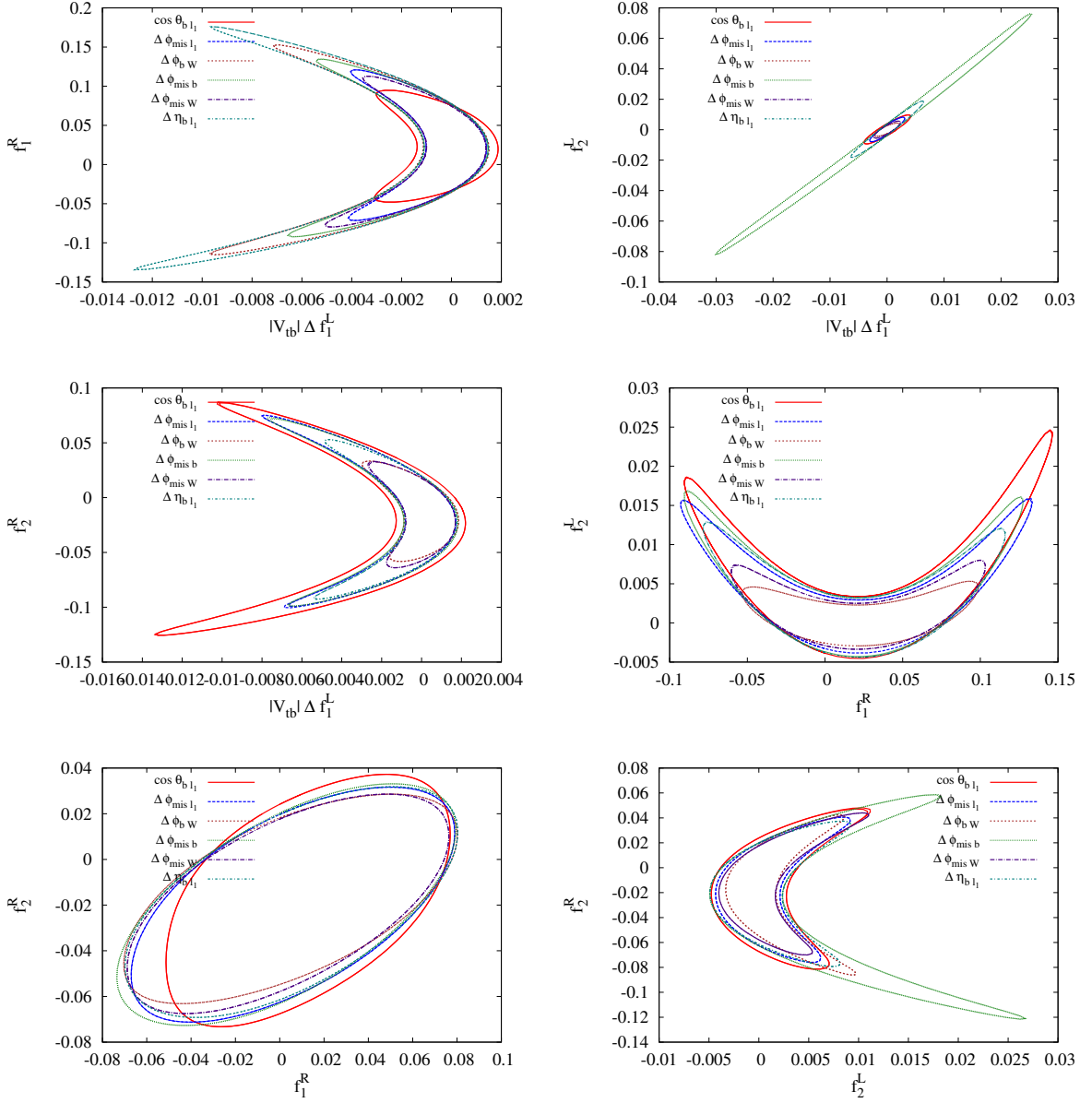


**Figure 9.** 68.3 % C.L. exclusion contours on the plane of  $|V_{tb}| \Delta f_1^L - f_1^R$ ,  $|V_{tb}| \Delta f_1^L - f_2^L$ ,  $|V_{tb}| \Delta f_1^L - f_2^R$ ,  $f_1^R - f_2^L$ ,  $f_1^R - f_2^R$  and  $f_2^L - f_2^R$  based on bin analysis for all kinematic observables in the leptonic decay mode of  $W^-$ .

### 3.3 Errors and correlations

In order to constrain the anomalous  $Wtb$  couplings  $f_i$  we further adopt the method of optimal observables by using the full information from the distribution of kinematic observables. In principle, for all anomalous couplings  $f_i$ , having a different shape profile, from each other, can constrain all of them simultaneously. For a given integrated Luminosity  $L$ , the statistical errors of the  $f_i$  and the correlations of the errors among the anomalous couplings measurement can be obtained from the  $\chi^2$  which is a function of all anomalous



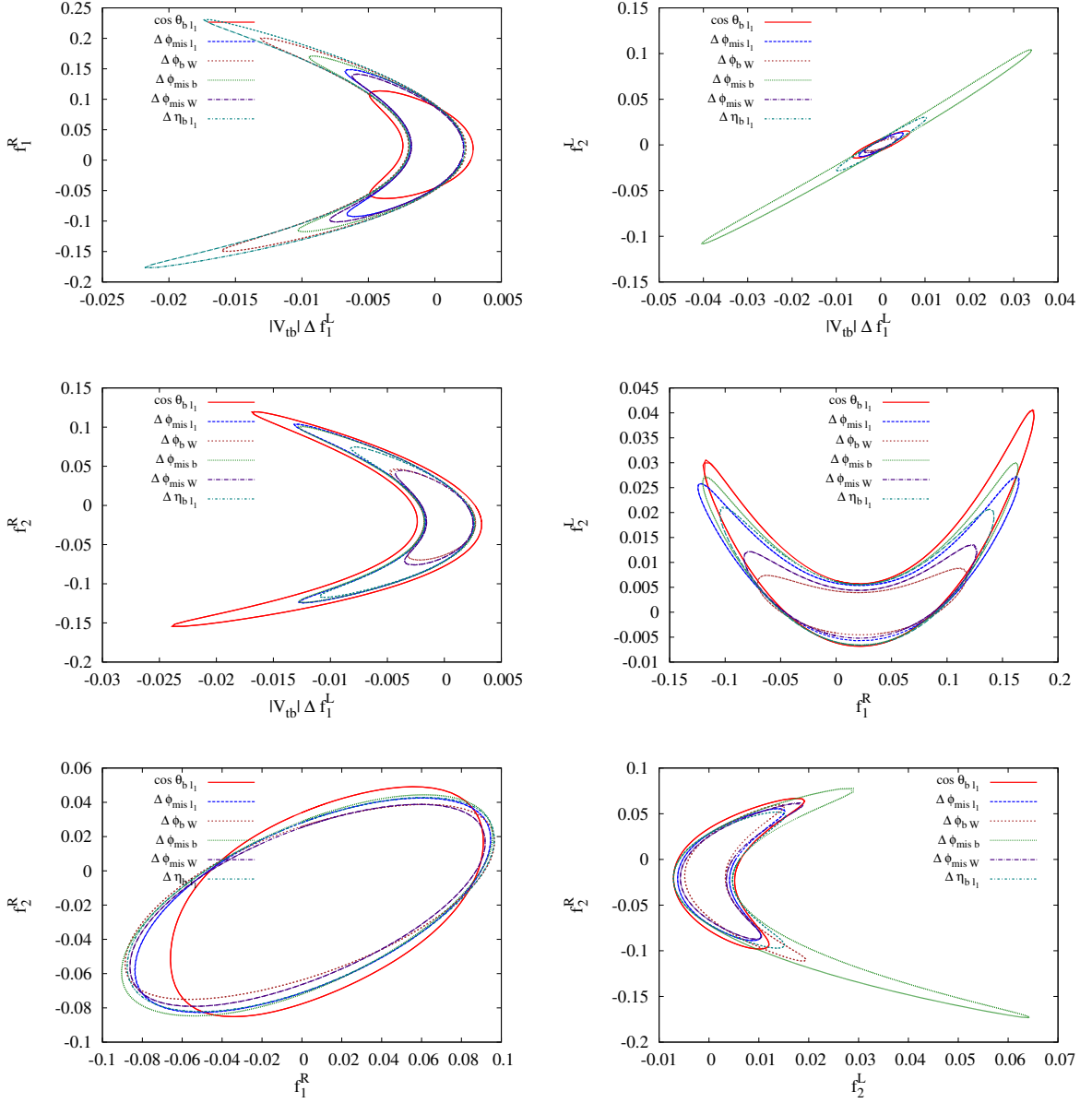


**Figure 10.** 95 % C.L. exclusion contours on the plane of  $|V_{tb}| \Delta f_1^L - f_1^R$ ,  $|V_{tb}| \Delta f_1^L - f_2^L$ ,  $|V_{tb}| \Delta f_1^L - f_2^R$ ,  $f_1^R - f_2^L$ ,  $f_1^R - f_2^R$  and  $f_2^L - f_2^R$  based on bin analysis for all kinematic observables in the leptonic decay mode of  $W^-$ .

couplings. Redefining the  $\chi^2$  of equation (3.6) in terms of the two anomalous couplings and the covariance matrix  $V$  we have

$$\chi^2(f_i, f_j) = \chi_{\min}^2 + \sum_{i,j} (f_i - \bar{f}_i) [V^{-1}]_{ij} (f_j - \bar{f}_j) \quad (3.9)$$

$V^{-1}$  can be evaluated using the approximation (3.7). If the SM prediction gives a reasonably good description of the data in most of the phase space region, then the statistical errors

$\Delta f_i$  of  $f_i$  and their correlations are determined solely in terms of the covariance matrices  $V$  as

$$f_i - \bar{f}_i = \pm \Delta f_i = \pm \sqrt{V_{ii}}, \quad \rho_{ij} = V_{ij} / \sqrt{V_{ii} V_{jj}}. \quad (3.10)$$

$\rho_{ij}$  gives correlation coefficient between two distinct anomalous coupling  $f_i$  and  $f_j$  and gives the absolute error for a given anomalous coupling  $f_i = f_j$ .  $\Delta f_i$  gives the uncertainty with which these couplings will be measured at LHeC.  $\bar{f}_i$  is the expected mean value in SM, which is zero for all the anomalous couplings  $f_i$ .

Subsequently, an optimal analysis for  $E_p = 7$  TeV and  $E_e = 60$  GeV with integrated luminosity  $L = 100 \text{ fb}^{-1}$  is made for all kinematic observables in both hadronic and the leptonic modes. The inverse of the covariance matrix  $V_{ij}^{-1}$  are generated from the each sensitive kinematic observables and we compute the corresponding respective correlation matrix. We also provide the accuracy with which the anomalous couplings can be measured from each of these distributions. The correlation matrices and the absolute error of each and every couplings for the hadronic modes are given here.

$$\begin{aligned}
& \Delta f_1^L = \pm 1.5 \times 10^{-4} \begin{pmatrix} 1 \\ 0 & 1 \\ .21 & 0 & 1 \\ 0 & .24 & 0 & 1 \end{pmatrix}; \quad \Delta f_1^L = \pm 1.2 \times 10^{-4} \begin{pmatrix} 1 \\ 0 & 1 \\ .07 & 0 & 1 \\ 0 & .20 & 0 & 1 \end{pmatrix}; \\
& f_1^R = \pm 2.3 \times 10^{-2} \quad f_1^R = \pm 2.1 \times 10^{-2} \\
& f_2^L = \pm 3.9 \times 10^{-3} \quad f_2^L = \pm 1.1 \times 10^{-3} \\
& f_2^R = \pm 1.6 \times 10^{-2} \quad f_2^R = \pm 1.1 \times 10^{-2} \\
& \qquad (a) \cos \theta_{\bar{b}j_1} \qquad \qquad \qquad (b) \Delta \phi_{\bar{b}W}
\end{aligned}$$

$$\begin{aligned}
& \Delta f_1^L = \pm 1.3 \times 10^{-4} \begin{pmatrix} 1 \\ 0 & 1 \\ .26 & 0 & 1 \\ 0 & .26 & 0 & 1 \end{pmatrix}; \quad \Delta f_1^L = \pm 1.4 \times 10^{-4} \begin{pmatrix} 1 \\ 0 & 1 \\ .35 & 0 & 1 \\ 0 & .24 & 0 & 1 \end{pmatrix}; \\
& f_1^R = \pm 2.2 \times 10^{-2} \quad f_1^R = \pm 2.2 \times 10^{-2} \\
& f_2^L = \pm 4.9 \times 10^{-3} \quad f_2^L = \pm 5.3 \times 10^{-3} \\
& f_2^R = \pm 1.6 \times 10^{-2} \quad f_2^R = \pm 1.5 \times 10^{-2} \\
& \qquad (c) \Delta \phi_{\not{E}_T \bar{b}} \qquad \qquad \qquad (d) \Delta \phi_{\not{E}_T j_1}
\end{aligned}$$

$$\begin{aligned}
& \Delta f_1^L = \pm 1.2 \times 10^{-4} \begin{pmatrix} 1 \\ 0 & 1 \\ .21 & 0 & 1 \\ 0 & .24 & 0 & 1 \end{pmatrix}; \quad \Delta f_1^L = \pm 1.1 \times 10^{-4} \begin{pmatrix} 1 \\ 0 & 1 \\ .30 & 0 & 1 \\ 0 & .24 & 0 & 1 \end{pmatrix}. \\
& f_1^R = \pm 2.2 \times 10^{-2} \quad f_1^R = \pm 2.0 \times 10^{-2} \\
& f_2^L = \pm 2.8 \times 10^{-3} \quad f_2^L = \pm 3.0 \times 10^{-3} \\
& f_2^R = \pm 1.5 \times 10^{-2} \quad f_2^R = \pm 1.5 \times 10^{-2} \\
& \qquad (e) \Delta \phi_{\not{E}_T W} \qquad \qquad \qquad (f) \Delta \eta_{\bar{b}j_1} \qquad \qquad (3.11)
\end{aligned}$$

The optimal analysis corresponding to the sensitive distributions for  $\Delta f_1^L, f_1^R, f_2^L$  and  $f_2^R$  (based on different asymmetries) for leptonic channels gives the following  $4 \times 4$  correlation

matrices:

$$\begin{aligned}
& \Delta f_1^L = \pm 6.7 \times 10^{-5} \begin{pmatrix} 1 & & & \\ & 1 & & \\ & .10 & 0 & 1 \\ & 0 & .18 & 0 & 1 \end{pmatrix}; & \Delta f_1^L = \pm 1.2 \times 10^{-4} \begin{pmatrix} 1 & & & \\ & 1 & & \\ & 0 & 1 & \\ & .06 & 0 & 1 \\ & 0 & .20 & 0 & 1 \end{pmatrix}; \\
& f_1^R = \pm 1.2 \times 10^{-2} \begin{pmatrix} 1 & & & \\ & 1 & & \\ & .10 & 0 & 1 \\ & 0 & .18 & 0 & 1 \end{pmatrix}; & f_1^R = \pm 2.1 \times 10^{-2} \begin{pmatrix} 1 & & & \\ & 1 & & \\ & 0 & 1 & \\ & .06 & 0 & 1 \\ & 0 & .20 & 0 & 1 \end{pmatrix}; \\
& f_2^L = \pm 9.8 \times 10^{-4} \begin{pmatrix} 1 & & & \\ & 1 & & \\ & .10 & 0 & 1 \\ & 0 & .18 & 0 & 1 \end{pmatrix}; & f_2^L = \pm 9.4 \times 10^{-4} \begin{pmatrix} 1 & & & \\ & 1 & & \\ & .06 & 0 & 1 \\ & 0 & .20 & 0 & 1 \end{pmatrix}; \\
& f_2^R = \pm 1.0 \times 10^{-2} \begin{pmatrix} 1 & & & \\ & 1 & & \\ & .10 & 0 & 1 \\ & 0 & .18 & 0 & 1 \end{pmatrix}; & f_2^R = \pm 1.1 \times 10^{-2} \begin{pmatrix} 1 & & & \\ & 1 & & \\ & 0 & 1 & \\ & .06 & 0 & 1 \\ & 0 & .20 & 0 & 1 \end{pmatrix}; \\
& \hspace{10em} (a) \cos \theta_{\bar{b}l_1} & \hspace{10em} (b) \Delta \phi_{\bar{b}W} \\
\\
& \Delta f_1^L = \pm 1.3 \times 10^{-4} \begin{pmatrix} 1 & & & \\ & 1 & & \\ & .23 & 0 & 1 \\ & 0 & .24 & 0 & 1 \end{pmatrix}; & \Delta f_1^L = \pm 1.2 \times 10^{-4} \begin{pmatrix} 1 & & & \\ & 1 & & \\ & .13 & 0 & 1 \\ & 0 & .22 & 0 & 1 \end{pmatrix}; \\
& f_1^R = \pm 2.2 \times 10^{-2} \begin{pmatrix} 1 & & & \\ & 1 & & \\ & .23 & 0 & 1 \\ & 0 & .24 & 0 & 1 \end{pmatrix}; & f_1^R = \pm 2.1 \times 10^{-2} \begin{pmatrix} 1 & & & \\ & 1 & & \\ & .13 & 0 & 1 \\ & 0 & .22 & 0 & 1 \end{pmatrix}; \\
& f_2^L = \pm 3.6 \times 10^{-3} \begin{pmatrix} 1 & & & \\ & 1 & & \\ & .23 & 0 & 1 \\ & 0 & .24 & 0 & 1 \end{pmatrix}; & f_2^L = \pm 2.1 \times 10^{-3} \begin{pmatrix} 1 & & & \\ & 1 & & \\ & .13 & 0 & 1 \\ & 0 & .22 & 0 & 1 \end{pmatrix}; \\
& f_2^R = \pm 1.5 \times 10^{-2} \begin{pmatrix} 1 & & & \\ & 1 & & \\ & .23 & 0 & 1 \\ & 0 & .24 & 0 & 1 \end{pmatrix}; & f_2^R = \pm 1.3 \times 10^{-2} \begin{pmatrix} 1 & & & \\ & 1 & & \\ & .13 & 0 & 1 \\ & 0 & .22 & 0 & 1 \end{pmatrix}; \\
& \hspace{10em} (c) \Delta \phi_{\not{E}_T l_1} & \hspace{10em} (d) \Delta \phi_{\not{E}_T W} \hspace{10em} (3.12)
\end{aligned}$$

## 4 Observations and conclusions

An attempt has been made to study and investigate the sensitivity of the measurement of anomalous  $Wtb$  couplings associated with the left or right vector and tensor chiral currents. LHeC being comparatively clean with respect to  $pp$  and  $p\bar{p}$  colliders, provides an excellent environment to study the electroweak production of single anti-top. We analyse the effect of anomalous couplings in the  $Wtb$  vertex by examining its one dimensional distributions. We summarise our observations as follows :

- (i) We observed high yields of single anti-top quark production and achieved fiducial efficiency of  $\sim 33\%$  and  $\sim 25\%$  in the hadronic and leptonic decay modes of  $W^-$  respectively after imposing selection cuts. They are shown in Tables 1 and 2 respectively.
- (ii) On studying the polarization distribution of  $W^-$  with the variation of the anomalous couplings from anti-top quark decay as depicted in the Figure 4, we find generically the negative helicity  $\mathcal{F}_-$  and positive helicity  $\mathcal{F}_+$  fraction of events show opposite trend with the variation of all anomalous couplings.  $\mathcal{F}_-$  is highly sensitive to the right handed tensor current while events with longitudinally polarized  $W^-$  bosons grows with the increase in the couplings corresponding to the left handed tensor and right handed vector currents.
- (iii) Asymmetries of kinematic variables are constructed from the one dimensional distribution as preliminary estimators for the sensitivity. It is found that asymmetries constructed from distributions can discriminate the effect of the vector and tensor chiral currents except for  $|V_{tb}| \Delta f_1^L$  as shown in Tables 3 and 4, provided the anomalous couplings are of the order of  $\sim 10^{-1}$ .
- (iv) We have conducted the  $\chi^2$  analysis based on the differential events of the kinematic observables and with systematic error  $\delta_{sys} = 2\%$  and an integrated luminosity of  $100 \text{ fb}^{-1}$  data. This gives us the exclusion contours at 68.3 % and 95 % C.L. on the six

different two dimension planes defined by the four anomalous couplings corresponding to the each of the six distinct kinematic observables. Contours are provided for both hadronic and leptonic decay modes of  $W^-$  in Figures 7, 8 and 9,10 respectively. From both hadronic and leptonic exclusion contours at 95% we find that the anomalous couplings  $|V_{tb}| \Delta f_1^L$  and  $f_2^L$  can be measured at the accuracy of  $\sim 10^{-3}$ . The right handed current however can be determined at the level of  $10^{-2}$  as the sensitivity comes from the new physics squared term and not the interference with SM unlike the left chiral currents.

- (v) Adopting the technique of the optimal observable we extract the inverse of the covariance matrices corresponding to each of the six kinematic observables by using the full information of all the four anomalous couplings in the  $\chi^2$  as defined by equation (3.9). Inverting these covariant matrices we derived the errors and their correlations for both the decay channels of  $W^-$  with an integrated luminosity of  $100 \text{ fb}^{-1}$  data corresponding to LHeC center of mass energy  $\sqrt{s} \approx 1.3 \text{ TeV}$ . Errors and correlation matrices are shown in equations (3.11) and (3.12) corresponding to the hadronic and leptonic modes respectively. We observe that the anomalous couplings associated with the left handed vector and tensor current can be measured with the accuracy of  $10^{-4}$  while those associated with the corresponding right handed currents are sensitive at the order of  $10^{-2}$ . Thus we show an improvement in estimating the couplings by one and two order of magnitude over the naive bin analysis and the angular asymmetries respectively.

Our analysis shows that we can probe the  $Wtb$  anomalous couplings at LHeC to a very high unprecedented accuracy which are comparable to those which exist from the indirect search of  $B$  meson decays.

We hope that our report will be useful in studying the physics potential of the LHeC project.

## Acknowledgments

SD, AG and MK would like to acknowledge the partial support from DST, India under grant SR/S2/HEP-12/2006. AG would like to acknowledge CSIR (ES) award for the partial financial support.

## References

- [1] G. L. Kane, G. A. Ladinsky and C. P. Yuan, Phys. Rev. D **45**, 124 (1992).
- [2] J. A. Aguilar-Saavedra, Nucl. Phys. B **812**, 181 (2009).
- [3] J. A. Aguilar-Saavedra, Nucl. Phys. B **821**, 215 (2009).
- [4] H. S. Do, S. Groote, J. G. Korner and M. C. Mauser, Phys. Rev. D **67**, 091501 (2003).
- [5] F. Larios, M. A. Perez and C. P. Yuan, Phys. Lett. B **457**, 334 (1999).
- [6] G. Burdman, M. C. Gonzalez-Garcia and S. F. Novaes, Phys. Rev. D **61**, 114016 (2000).

- [7] E. Barberio *et al.* [Heavy Flavor Averaging Group (HFAG) Collaboration], arXiv:0704.3575 [hep-ex].
- [8] B. Grzadkowski and M. Misiak, Phys. Rev. D **78**, 077501 (2008) [Erratum-ibid. D **84**, 059903 (2011)].
- [9] V. M. Abazov *et al.* [D0 Collaboration], Phys. Rev. Lett. **100** (2008) 062004.
- [10] V. M. Abazov *et al.* [D0 Collaboration], Phys. Rev. Lett. **103**, 092001 (2009).
- [11] CDF/PUB/TOP/PUBLIC/10793
- [12] S. Chatrchyan *et al.* [CMS Collaboration], JHEP **1212**, 035 (2012).
- [13] G. Aad *et al.* [ATLAS Collaboration], Phys. Lett. B **717**, 330 (2012).
- [14] V. M. Abazov *et al.* [D0 Collaboration], Phys. Lett. B **713**, 165 (2012).
- [15] B. Sahin and A. A. Billur, Phys. Rev. D **86**, 074026 (2012).
- [16] J. A. Aguilar-Saavedra, J. Carvalho, N. F. Castro, F. Veloso and A. Onofre, Eur. Phys. J. C **50**, 519 (2007).
- [17] ATLAS-CONF-2011-037
- [18] J. A. Aguilar-Saavedra, N. F. Castro and A. Onofre, Phys. Rev. D **83**, 117301 (2011).
- [19] K. Ciekiewicz and K. Kolodziej, Acta Phys. Polon. B **34**, 5497 (2003).
- [20] B. Grzadkowski and Z. Hioki, Phys. Lett. B **557**, 55 (2003).
- [21] S. D. Rindani, Pramana **54**, 791 (2000).
- [22] Alwall:2011uj K. Kolodziej, Phys. Lett. B **584**, 89 (2004).
- [23] S. Atag, O. Cakir and B. Dilec, Phys. Lett. B **522**, 76 (2001).
- [24] J. L. Abelleira Fernandez *et al.* [LHeC Study Group Collaboration], J. Phys. G **39**, 075001 (2012).
- [25] J. L. Abelleira Fernandez, C. Adolphsen, P. Adzic, A. N. Akay, H. Aksakal, J. L. Albacete, B. Allanach and S. Alekhin *et al.*, arXiv:1211.4831 [hep-ex].
- [26] O. Bruening and M. Klein, Mod. Phys. Lett. A, Vol. 28, No. **16**, 1330011 (2013).
- [27] A. Senol, Nucl. Phys. B **873**, 293 (2013).
- [28] S. S. Biswal, R. M. Godbole, B. Mellado and S. Raychaudhuri, Phys. Rev. Lett. **109**, 261801 (2012).
- [29] T. Han and B. Mellado, Phys. Rev. D **82**, 016009 (2010).
- [30] J. L. Abelleira Fernandez *et al.* [LHeC Study Group Collaboration], arXiv:1211.5102 [hep-ex].
- [31] S. Dutta, A. Goyal and M. Kumar, Phys. Rev. D **87**, 094016 (2013).
- [32] I. T. Cakir, A. Senol and A. T. Tasci, arXiv:1301.2617 [hep-ph].
- [33] I. T. Cakir, O. Cakir and S. Sultansoy, Phys. Lett. B **685**, 170 (2010).
- [34] J. Alwall, M. Herquet, F. Maltoni, O. Mattelaer and T. Stelzer, JHEP **1106**, 128 (2011).
- [35] A. Alloul, J. D'Hondt, K. De Causmaecker, B. Fuks and M. R. de Trautenberg, Eur. Phys. J. C **73**, 2325 (2013).